

Engineering insect flight metabolics using immature stage implanted microfluidics†

Aram J. Chung and David Erickson*

Received 29th August 2008, Accepted 31st October 2008

First published as an Advance Article on the web 24th November 2008

DOI: 10.1039/b814911a

Small-scale insect inspired aircraft represent a promising approach to downscaling traditional aircraft designs. Despite advancements in microfabrication, however, it has proven difficult to fully replicate the mechanical complexities that enable these natural systems. As an alternative, recent efforts have used implanted electrical, optical or acoustic microsystems to exert direct control over insect flight. Here we demonstrate, for the first time, a method of directly and reversibly engineering insect flight metabolics using immature stage implanted microfluidics. We present our technique and device for on-command modulation of the internal levels of L-glutamic and L-aspartate acids and quantify the resulting changes in metabolic activity by monitoring respiratory CO₂ output. Microfluidic devices implanted 1 to 2 days prior to insects' emergence achieved survivability and flight-capable rates of 96% and 36%, respectively. Behavior ranging from retarded motion to complete, reversible paralysis, over timescales ranging from minutes to hours is demonstrated.

Introduction

Micro-air-vehicles (MAVs) are small aircraft with a maximal wingspan of approximately 15 cm and flight speed below 10 m s⁻¹.¹ Such systems are of significant interest to the military, industrial and academic communities largely as a result of their potential to perform bio-chemical sensing in hazardous locations, long-range surveillance and stealthy reconnaissance.² Rapid progress in micro-electro-mechanical-systems (MEMS)^{3,4} technology (including power generation, energy storage, communications, sensing, and subcomponent assembly) has enabled further miniaturization and improved performance in these systems, however, to date they still suffer from small payload capacity, large size or poor flight stability, and short operational time.⁵⁻⁷ The latter of these is a particularly important limitation and results from the technical challenges involved in creating a compact and lightweight high-density power source with a sufficiently long lifetime.^{8,9}

As a result of the challenges in downscaling traditional aircraft designs, a number of researchers have looked to the natural world to develop bio-inspired MAVs;¹⁰ for instance mimicking the body shapes, wing shapes and flapping patterns that are

present in nature.¹¹⁻¹⁶ Emulating the vast complexity of nature, however, has proven to be an extremely difficult engineering problem and thus man-made systems are unlikely to outperform natural flyers (particularly in terms of flight dynamics and power efficiency) in the near future. Flying insects, for example, have evolved an aerodynamic shape that allows them to remain stable in turbulent air conditions and a complex wing flapping motion with an extremely energy efficient stroke.¹⁷ Many insects spend the majority of their pre-adult lives constantly feeding in order to store sufficient energy (in the form of glucose) to sustain them throughout their adult lives. Additionally, large flying moths such as *Manduca sexta* or *Ascalapha odorata* are able to carry payloads well in excess of one gram without significant degradation of their natural flight mechanics.^{18,19}

The ability of flying insects to meet or exceed the performance capabilities of current MAVs has led to recent interest in integrating MEMS technology with these living systems in order to exert some level of flight control over them. Bozkurt *et al.*^{20,21} for example, reported direct electrical control over the flight of a *Manduca sexta* (*M. Sexta*) moth by implanting micro-fabricated electrical probes at the pupal stage. In that work the probes were used to send biphasic electrical pulses into the flight muscles enabling effective control over wing motion. They demonstrated down- and up-stroke actuation of each wing separately, which affected the flight direction of the moth. Also using electrical stimulation, Sato *et al.*²² demonstrated control over beetle flight using an implanted and tetherless microsystem and Ando and Kanzaki²³ presented longitudinal control in freely flying hawkmoths. Recently, Ritzmann *et al.*²⁴ demonstrated the possibility of controlling the locomotor activity of a cockroach using brain nerve group stimulation. With the aim of developing a technique for powering these devices, Reissman and Garcia²⁵ recently presented a power harvesting system aimed at extracting energy from the natural vibrations that occur during insect flight using surgically inserted piezoelectric materials and inductor-coils.

Sibley School of Mechanical and Aerospace Engineering, Cornell University, Ithaca, NY, 14853, USA. E-mail: de54@cornell.edu; Fax: +1 607-255-1222; Tel: +1 607-255-4861

† Electronic supplementary information (ESI) available: Five illustrative movies and three figures are included here as part of this work. Movie 1 shows an overview of the pupal stage implantation of the microfluidic device and subsequent successful emergence. Movie 2 shows the injection experiment used to determine the optimal drug, dosage and delivery site. Movie 3 demonstrates control of insect flight metabolics using microfluidics and Movie 4 illustrates the custom made agitator used to mechanically stimulate a continuous flight response. Lastly, Movie 5 demonstrates our control over insect flight metabolic while the insect is in the respirometry chamber used to measure the CO₂ output. Fig. S1 and S2 illustrate the determination of the optimal implantation, and Fig. S3 shows poor flight capability moths. See DOI: 10.1039/b814911a

Here we demonstrate a more intimate method of exerting control over insect flight, exploiting the use of immature stage implanted microfluidics to reversibly engineer the rate of flight metabolism. In this paper we present our technique for modulating the internal levels of a series of different chemicals known to affect the insect nervous system (specifically L-glutamic and L-aspartate acids) and thereby demonstrate dynamic control over metabolic output using microfluidics. In this study we use *M. sexta* moths as our model species due to its large potential payload capacity and excellent flight capability. The insect has a large body mass (~2 g), a wingspan of 10 cm and a potential flight range of kilometres. In addition to demonstrating the technique, we present here details of the implantation surgeries, injection experiments and microfluidic device. Changes in the rate of metabolic activity are quantified using a novel flight stimulation apparatus and by monitoring changes in CO₂ output. We demonstrate the ability to provide rapid chemical paralysis (from full flight activity to no motion) which lasts for several hours. Partial insect recovery is observed after 3 h with full recovery in less than 22 h. We propose that the system is the first step towards the development of an artificial insect nervous system.

Materials and methods

In this materials and methods section we begin with a detailed description of the implantation, injection process, device fabrication, and assembly procedure. The final subsection describes the respirometry system used to determine resting metabolic rate. All relevant animal care and use guidelines were followed in this study.

Implantation process

The microfluidic devices were implanted in *M. sexta* pupae, approximately 1 or 2 days before the adult insects were scheduled to emerge. Prior to the surgery, the pupae were placed on ice for approximately 25 min to minimize their movement and lower the inner body pressure. Using a sterilized scalpel, the dorsal exoskeleton and body skin were cut away and the device was partially implanted into the thorax near the dorsolongitudinal flight muscles (dl muscle). During implantation the device is gently inserted into the thorax to minimize the disruption to the aorta which passes nearby. To seal the wounds after surgery a viscous and fast curing biocompatible glue (Loctite® 454: ISO 10993, Henkel) was used. The rapid curing of the glue prevented penetration into body.

Injection process

A number of different chemicals were tested to gauge their effectiveness in generating the desired physiological response given the limitations outlined in the text. To gauge their performance, direct injection experiments were conducted by first folding the wings then inserting a needle (700 series syringes, Hamilton) containing the test drug into different locations along the insect (specifically the dorsal/ventral thorax, the head and every segment of the abdomen). The following chemicals were tested in various different concentrations and dissolved with 10 mM phosphate buffered saline (pH 7.4): γ -aminobutyric acid

(Sigma-Aldrich), taurine (Sigma-Aldrich), β -alanine (Sigma-Aldrich), atropine (Sigma-Aldrich), Malathion (Sigma-Aldrich), scorpion venom (*Hadrurus arizonensis*, Spider Pharm), L-aspartate acid potassium salt hemihydrates (Sigma-Aldrich), and L-glutamic acid potassium salt monohydrate (Sigma-Aldrich). The insect response was gauged visually.

Microfabrication

The microfluidic device presented here consists of three layers; a silicon layer contained the microwell and the upper set of electrodes, Parylene deposited PDMS macro reservoir, and a Pyrex bottom substrate which served to seal the reservoir and hold the lower electrode. The top silicon layer was fabricated using the same methods as described previously by Chung *et al.*²⁶ Briefly, silicon nitride was deposited on both sides of the (100) n-doped silicon wafer and the backside was etched to define the location of the wells. Following this, gold electrodes were evaporated and patterned, and then a polyimide dielectric layer was spun and etched. The microwells were then defined by immersing the wafer in KOH and the remaining silicon nitride underneath the gold membrane was removed by reactive ion etching. To create the PDMS macro reservoir, a 10 : 1 (base : linker) mixture of PDMS was cured at 80 °C for 60 min, and the final structure was cut out, and then placed on the microscope slide glass. Transparent 3M scotch® tape was attached on top of the PDMS structure which allows the deposition of Parylene only at the sidewalls of the reservoir. The PDMS surface was modified by oxygen plasma prior to the Parylene deposition in order to improve the adhesion between Parylene and PDMS.^{27,28} Following this, 1 μ m thick Parylene (Parylene C, Specialty Coating Systems) was deposited using a Parylene deposition tool (PDS 2010 Labcoter, Specialty Coating Systems), and then the scotch® tape was removed. Lastly, to fabricate the bottom Pyrex layer, 10 nm/100 nm layers of titanium/gold were evaporated and patterned using an image reversal contact lithography process to form the electrode pads and leads.

Microchip assembly

The upper (silicon), the middle (PDMS), and the bottom (Pyrex) substrates were placed in conformal contact with each other and bonded together by the plasma treatment and cured in the 80 °C oven overnight. After the microchip assembly, a PEG (polyethylene glycol) film was coated on the entire surface of the assembled device using a molecular vapor deposition tool (MVD 100, Applied MicroStructures) to minimize the physiological response since PEG deposition is a well known biocompatible surface molecular modification.²⁹ The microwell and macro reservoir were filled with different chemicals using a microlitre syringe (NanoFil™, World Precision Instrument) through the slit, sealed with biocompatible wax (Butler GUM, Sunstar). The final fully loaded device weighs approximately 0.3 g, which is 15% of the total insect's body mass and the payload capacity.

Respirometry to determine resting metabolic rate

Metabolic rates were measured using a flow-through respirometry chamber. The insect ventral thorax was glued onto a narrow beam and the stage was mounted inside of the chamber. Dry,

CO₂ free air was sent through the 3 litre respirometry chambers, first for 5 min to set up the baseline for the resting metabolic rate, and then the insect was mechanically stimulated to initiate a flight response (which will be described more in the “Quantification of the metabolic rate” section below). To measure the continuous changes in CO₂ level reflective of the metabolic output of the insect, all the air from the jar passed through the carbon dioxide analyzer (Li-Cor 6252, Lincoln), and data were collected.

Results and discussions

Implantation

As shown in Fig. 1, the microfluidic device is partially implanted within the *M. sexta* dorsal thorax at the pupal stage of development. Consistent with the ideas described in Bozkurt *et al.*^{20,21} and used in Paul *et al.*,³⁰ implantation is done at an immature developmental stage. The reason for this is that wounds which occur during the implantation surgery are known to heal better during the natural molting process.^{30–32} It is expected that this results in a smaller physiological footprint, since the device has been carried through a greater portion of the insect’s

development. Earlier works^{22–24,33} have relied on adult stage implantations. Fig. 1a outlines the *M. sexta* lifecycle, illustrating the stage in its development at which the implantations done here were conducted. To determine the optimal implantation strategy that minimizes the physiological footprint and maximizes survivability, we performed a number of insertion experiments varying the timing of the implantation (see Fig. S1 in supplemental material)[†] and location (see Fig. S2 in supplemental material).[†] We chose to conduct implantation at two different time periods, relatively early (approximately 1 week prior to emergence) and relatively late (1–2 days prior to emergence). As shown in the supplemental material test implants were conducted at numerous different parts of the body. The impact of the implants was gauged visually post emergence by noting which insects exhibited malformed extremities (wings) or poor flight characteristics. We define a system with “poor flight capability” as one which exhibits some retarded ability to flap its wings. These problems tended to be caused by two main factors. Although most moths survived the insertion surgeries under healthy conditions, in many cases the implanted devices hindered the adult moths ability to pull themselves out from the cuticle during emergence. The result was deformed wings clearly unable to be used for flight (see Fig. S3).[†] The second cause

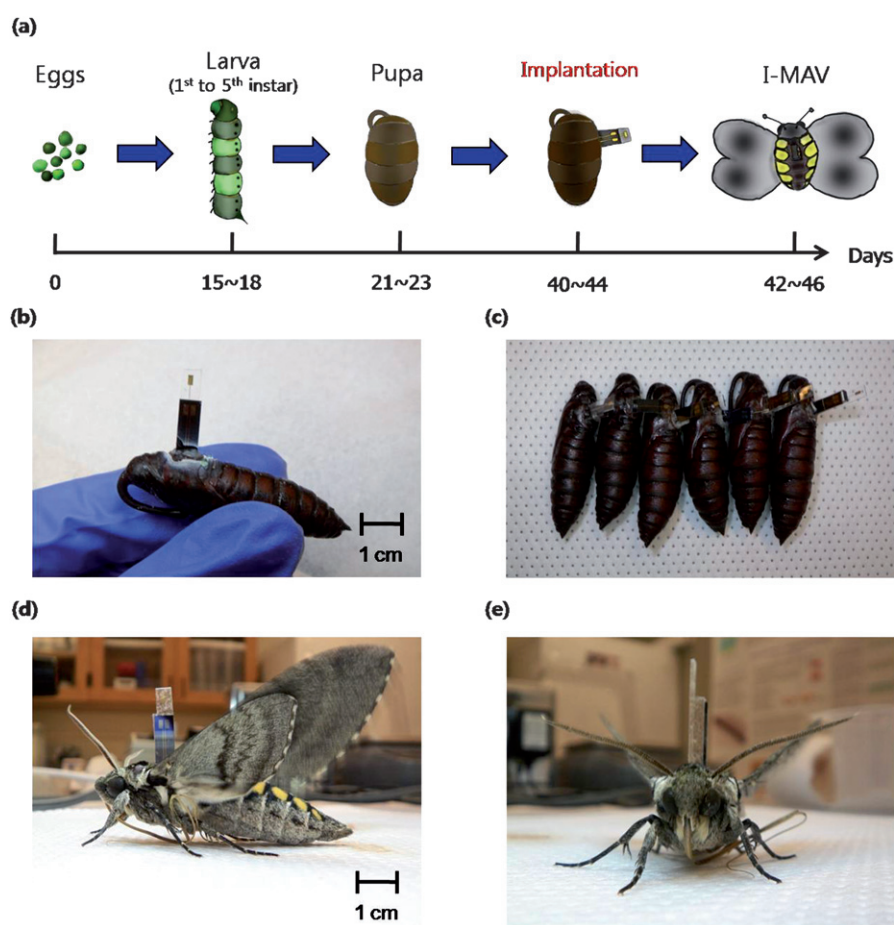


Fig. 1 (a) A schematic view of the developmental stages of a *M. sexta* moth. Insertion of the microfluidic device is conducted at the pupal stage of development. (b and c) Device insertion surgeries are done in the dorsal thorax with the microfluidic chip inserted approximately 5 mm into the pupa. Then wound is sealed with biocompatible glue. (d and e) *M. sexta* moth successfully emerged with an implanted device.

Table 1 Comparison of survivability rate depending on the implantation date

Survivability data	7–8 days	1–2 days
Survivability rate	93.75%	96.0%
Flight-capable insect rate	12.5%	36.0%
Sample size	32	50

tended to be damage to the dorsolongitudinal flight muscles during implantation. This limited the wing stroke which could be exerted during flight.

Based on these results, we found that the dorsal thorax is the best location for implantation, and 1 to 2 days prior to the insects' emergence is the best timing for our current design as indicated in Table 1. A movie illustrating the implantation surgery and developmental process is available as supplemental material.† Fig. 1d and 1e show a successfully emerged flight-capable insect. Paul *et al.*³⁰ presented results on inserting of silicon chips in the pupal stage with the flight-capable moths rate of 87.5%. The devices implanted here were much larger and heavier devices resulting in survivability and flight-capable insect rates of 96% and 36%, respectively (total sample size was 50). As can be seen in Table 1, the survivability remains high in both cases suggesting that the implantation date does not critically affect the insects' life. The flight-capable rate however strongly depends on the insertion date with the latter implants yielding more flight ready insects. The increase in flight ready rate observed for the later implantations is likely due to the fact that since more of the insect is formed, the likelihood of damaging the flight muscles is less than in the earlier stage implants. With the more developed insect's the surgery could also be performed more precisely. At least part of the relatively low flight ready rate for the early stage implants is likely due to the relatively large size of the microfluidic device relative to that of the insect (as shown in Fig. 1). We are currently working on designs which reduce the physiological footprint of the device.

Characterization of physiological response to chemical injection

Direct injection experiments were conducted to determine the optimal drug, dosage and delivery site for inducing the fastest physiological response and most complete but reversible impact on the level of observable insect activity. Fig. 2 shows the injection procedure (see also Movie 2).† The maximum capacity of our microfluidic chip was 15 μL and thus this was considered the upper limit for our injection volumes.

For the species of interest here, there are three candidate injection sites: the head, thorax and abdomen. The microfluidic device used here is larger than the insect's head and thus this was removed as a candidate. Numerous injections were carried out at various positions along the abdomen. It was generally observed that physiological response times were slower and the required dosage was higher (approximately 5 times) than for similar injections made in the thorax. We expect that the rapid response was a result of the proximity of the central nervous system (CNS) and heart (aorta) to the thorax injection site. As such the thorax was selected as the optimal injection/implantation site. Once the injection site was localized a large number of different chemicals

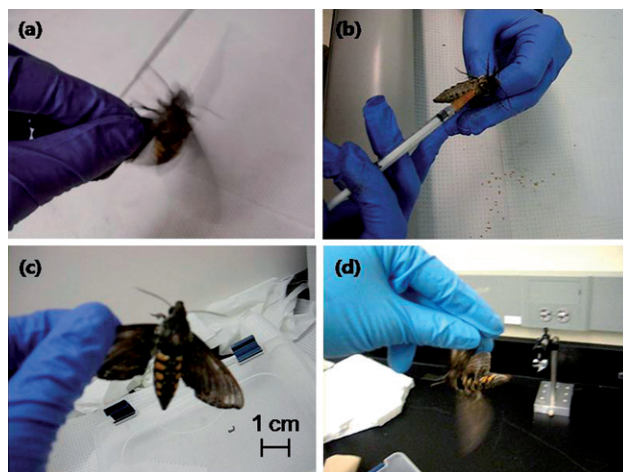


Fig. 2 Injection procedure. (a) Prior to injection the insect was stimulated to gauge its baseline activity level. (b) Various chemicals were injected into the thorax to determine the dosage effects on the degree and length of insect temporary paralysis. (c) The moth is paralyzed about a minute after injecting 5 μL of LGA. (d) In a successful test, after two to three hours, the moth recovers sufficiently to flap its wings.

and dosages were tested including components of spider, wasp and scorpion venom, and some insecticides.

The chemicals (L-glutamic acid (LGA), L-aspartate acid (LAA), γ -aminobutyric acid (GABA), taurine and β -alanine) that were found to enable successful reanimation of the insect, were the neurotransmitters that form the major/minor components of many spider and wasp venoms. We selected these chemicals because they tended to reversibly paralyze the insect by acting on the neuronal receptors, neuronal ion channels or synaptic membrane.³⁴ For example, GABA affects the insect's chloride ion channel to induce immobilization and LGA/LAA influences the synaptic membrane, binding site and physiologic receptors to cause paralysis.^{34,35} The reversibility of the inhibition can be explained in terms of the effect of the venom on the site which does not damage or destruct the synaptic membranes (reversed by a membrane dilution-washing procedure).³⁵ The excitation, therefore, decreases as time goes so that the reanimation of the activity can be found as we observed. The insecticide Malathion was found to instantly kill the insect even in small doses and thus was not considered a useful candidate for further study.

Table 2 gives details of chemicals used, the minimum volume required to achieve paralysis and remarks on the ability of the insect to recover (all injections done in the thorax). As can be seen, the approach most effective at retarding insect motion was a 5 μL solution of 5.9 M LGA and 11.1 M solution of LAA (both chemicals are excitatory transmitters at insect skeletal neuromuscular junctions³⁶). These concentrations represented the saturation concentrations for these chemicals. In both cases within a minute of injection, the insect was immobilized for approximately 2 h, after which it regained its pre-injection activity level (supplementary Movie 2).†

Electrokinetic drug delivery device

The microfluidic device structure used here is a modification of that presented by Chung *et al.*,²⁶ which exploited the same

Table 2 List of chemicals injected into the thorax for immobilization

Chemical type (concentration)	Minimum volume	Remark
LAA (11.11 M)	>5 μL	Successful reanimation
LGA (5.9 M)	>5 μL	Successful reanimation
GABA (10 M)	>20 μL	Successful reanimation
Taurine (0.5 M)	>100 μL	Successful reanimation
β -Alanine (3 M)	>100 μL	Successful reanimation
Malathion (1.23 g L ⁻¹)	<1 μL	Insect did not survive
Atropine (N/A)	N/A	Insoluble in PBS
Hadrurus arizonensis (N/A)	N/A	Insoluble in PBS

electrochemical dissolution technique and electroactive ejection schemes. In the first stage, an electric potential is applied between two electrode pads on top of the microchip serving to electrochemically dissolve the membrane. To electrokinetically eject the contents from the reservoir, in the second stage a potential field is applied between one of the upper electrodes and that on the Pyrex bottom substrate. As described in detail in Chung *et al.*,²⁶ the technique is based on exploiting highly localized electrokinetic transport to rapidly exchange the contents of the reservoir with the external environment. The use of electrokinetic transport allows for a significant reduction in the amount of time required to eject the well contents over earlier diffusive transport based devices³⁷ (from hours to minutes), simplifies device design since only electrical components are required, and minimizes the rate amount of energy required per injection. As illustrated in Fig. 3, compared to our previous design²⁶ this device had an additional Parylene coated on-board poly(dimethylsiloxane), PDMS, reservoir to increase the injectable volume from 100 nL to approximately 15 μL . Due to water vapor permeability of the PDMS,³⁸ Parylene was deposited on the sidewalls of the PDMS reservoir. To improve the mechanical stability of the device, Pyrex glass was used as the bottom layer (as opposed to PDMS). These latter two improvements resulted in significant improvements in device lifetime (earlier designs had a lifetime of approximately 5 days). Long term tests of the device were not conducted, however, it was found that in all cases they remained operable for at least the expected lifetime of the insect.

To illustrate the electrokinetic transport processes involved in the ejection stage, a finite element model of the system was

constructed and simulated using the COMSOL finite element package. The computational domain used here matched exactly that shown in Fig. 3, comprising of both the well, PDMS reservoir and an exterior domain. Details of the modeling procedures and general assumptions are available in earlier works²⁶ and thus here we focus on the specifics of this implementation. Fig. 4 shows a two dimensional cut view of the transient convection-diffusion solution during the ejection process. To mimic the actual ejection process we consider pure electroosmotic flow. From Fig. 4 it can be seen that the applied potential induces a strong electroosmotic flow dragging fluid from the external environment into the reservoir. This then displaces the contents of the reservoir which is ejected through the middle of the outlet. Note that although some of it remains for the entire duration of the ejection process, much of the contents are ejected in the early stages. As we will show in the following section, the initial discharge in the first 90 s is sufficient to observe a response.

Demonstration of flight metabolism control using implanted microfluidics

Based on the results of the insertion experiments, the microfluidic devices were implanted in *M. sexta* pupae, approximately 1 or 2 days before the adult insects were scheduled to emerge. On-chip reservoirs were filled with one of three different chemicals, LGA, LAA, and phosphate buffered saline (PBS) buffer solution which served as a negative control. Flight metabolism control experiments and the quantification which will be described below were conducted only on moths which were capable of flight after

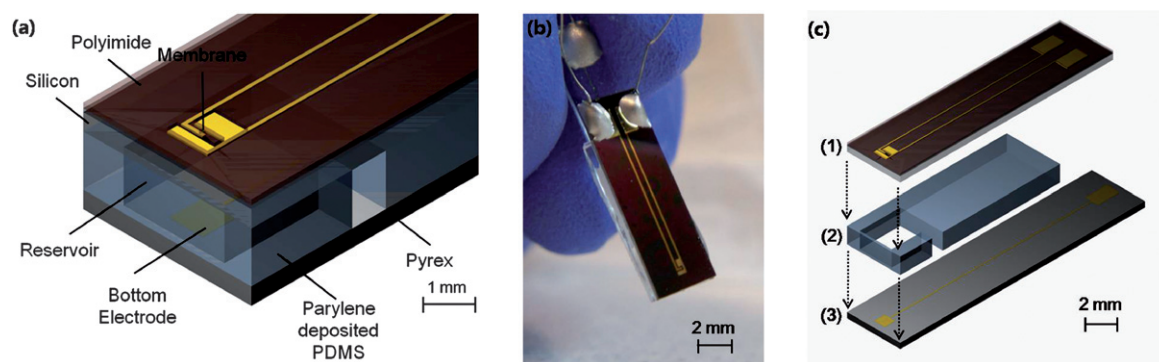


Fig. 3 (a) Schematic of the electroactive microwell drug delivery system developed here. (b) Fabricated and assembled electrokinetic microfluidic devices used here. The devices measure $4 \times 22 \times 2.5$ mm and weigh 250 mg. (c) Microchip assembly: (1) an upper silicon based structure, (2) Parylene deposited PDMS reservoir, and (3) electrically functionalized Pyrex bottom substrate are bonded together by the plasma treatment.

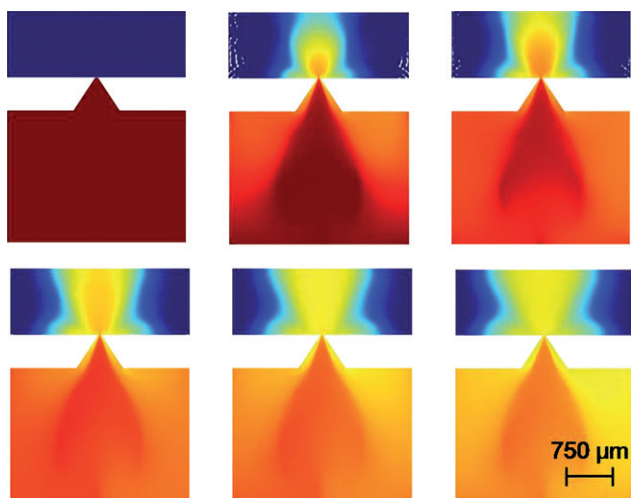


Fig. 4 To illustrate the electrokinetic transport processes involved in the ejection stage, a finite element analysis of time-dependent species transport of the system is shown. Images show cut view of species concentration every 60 s up to 300 s after the ejection process when 15 V is applied. In the color scheme shown here, the blue contours represent lower concentrations and the red contours higher ones.

emergence. A typical experiment is shown in Fig. 5, where as can be seen, the electrical leads from the device were connected to thin copper wires which lead to an overhanging boom supporting the insect in midair. All insects received only one injection (no multiple injection experiments were conducted). When a dosage command was issued, the two stage injection process (described above) was initiated. We applied 15 V for 4 min and 20 V for 4 min for membrane dissolution and electrokinetic ejection stages, respectively. For both LGA and LAA a dramatic reduction in the wing motion (*i.e.* rate and amplitude of flapping strokes) was observed, 90 s after the 2nd stage command was issued. No observable difference was found for the PBS ejection experiments. In the negative control case the device was excised to visually confirm that it had been actuated. During the ejection process, the applied potentials may have lead to some ohmic heat generation which could have affected the potency of the chemicals used during the injection process. Though we have not fully characterized this, we do not expect that this is significant since the results of the device and manual ejections yielded similar

results. After the discharging of the applied potential, the drug-induced immobilization lasted 1 h and 20 min, after which the moths regained activity level (see Movie 3).† The timescale for reanimation is much larger than that of immobilization because the insect regains its previous activity by natural recovery process. To verify that the paralysis was not due to the applied potential, the same voltages were applied on a dummy chip. As expected, no immobilization was noticed.

Quantification of the metabolic rate

To quantify the immobilization/reanimation process, metabolic rates were inferred from the carbon dioxide (CO₂) output of the insects in a respirometry chamber. Details of the experiment are available elsewhere^{39,40} and here we just briefly provide an overview of the experimental procedure. The moths were glued onto a narrow beam that allowed unencumbered wing flapping and leg movements. To stimulate a continuous flight response of the insect, a custom made mechanical agitator (Movie 4)† was placed inside of the sealed chamber. In the experiment, dry, CO₂ free air was pumped through the respirometry chamber at room temperature and all output gas passed through a carbon dioxide analyzer to measure the CO₂ output. Metabolic rate (and therefore CO₂ output) is higher during flight or attempted flight relative to periods when the animal was quiescent in the respirometry chamber.⁴⁰ To establish a baseline of the insect metabolic output at rest, the system was flushed until a stable CO₂ level was recorded. Following this the insect was mechanically stimulated as described above to initiate a flight response which was maintained until the CO₂ output again reached an equilibrium level. After 17 min of flight level activity, the membrane dissolution and ejection potentials were applied for approximately 10 min. Note that we applied the electric potential for this long of a time period here in order to be able to accurately gauge its effect on the insect activity level.

As can be seen in Fig. 6a the metabolic rate drops off rapidly following the LGA (5.9 M) ejection. The insect was stimulated for 10 s every 5 min until the 2 h mark with almost no activity observed (Movie 5).† At 45 to 47.5 min, to ensure the full immobilization, extremely strong perturbations were applied and the insect responded for a short time, approximately 1 min, but returned to its quiescent state immediately afterwards. To validate the reversibility of the process, 3 h and 22 h after the initial

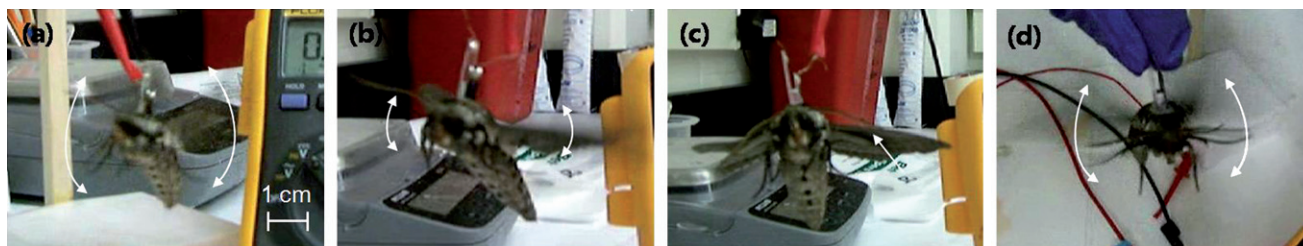


Fig. 5 Microfluidically modulated insect activity. (a) The overhanging boom supports the insect in midair allowing it to flap its wings unimpeded. (b) Actuation of the drug delivery device occurs in two stages. In the first stage an electric potential is applied between two electrode pads on top of the microchip serving to electrochemically dissolve the membrane. To electrokinetically eject the contents from the reservoir, in the second stage a potential field is applied between one of the upper electrodes and that on the Pyrex bottom substrate. Due to the ejection of the drug (here LGA), the activity of the wing motion decreases. (c) Insect fully immobilized by LGA in 90 s after 2nd stage command is issued. (d) After 1 h and 20 min, the moth is again able to flap its wings.

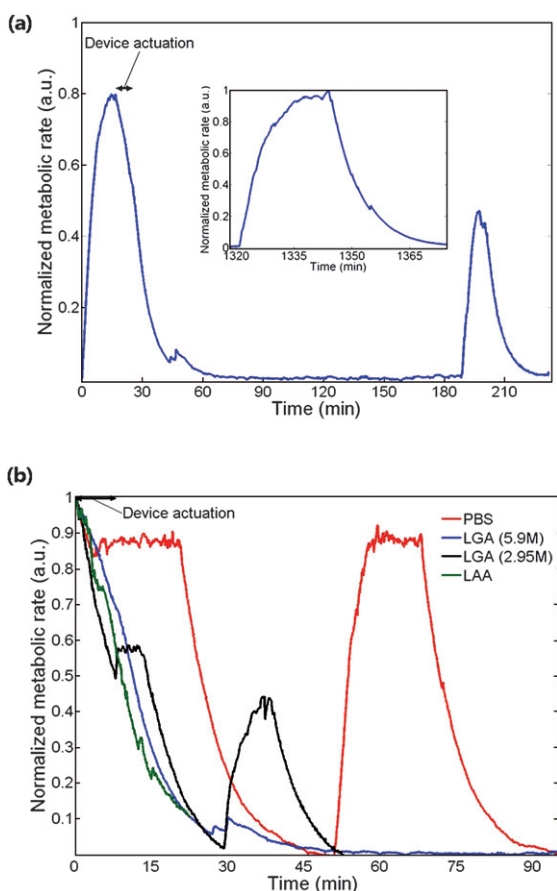


Fig. 6 (a) Representative recording of CO₂ emission from adult moth as a function of time when an implanted microfluidic device with 15 μ L of 5.9 M LGA was injected. (Inset) After 22 h, the insect was stimulated to fly for 25 min and it fully recovered its previous metabolic activity rate. (b) Normalized metabolic rate comparing 5.9 M LGA (blue), 2.95 M LGA (black), 11.1 M LAA (green) and PBS buffer (red).

ejection, the insect was again stimulated. At 3 h the insect was shown to recover 63.6% of its previous activity level (peak-to-peak value), and after 22 h the moth fully recovered its previous level (see inset in Fig. 6a).

Fig. 6b compares the result obtained for implanted devices containing different LGA doses (5.9 M from Fig. 6a and 2.95 M), LAA (11.1 M) and the negative control solution (PBS). The additional experiments were conducted using the same methodology and drug volume as described above. For more accurate comparison in this figure, we set time equals zero as the time when the device was actuated. When a half concentration dose of LGA (2.95 M) was injected, the metabolic rate dropped approximately 50%. When the agitator was reengaged, the insect resumed flight but only at this reduced activity level. The effect of LAA was similar to the full LGA dose, showing rapid immobilization and reanimation later as expected. When the negative control was ejected the insect continued to exhibit a strong flight response until the agitator was disengaged at 20 min. At 50 min the agitator was turned on again and the insect resumed full activity. This result demonstrates that the flight response of the insect can be directly manipulated through dosage control.

Summary and conclusion

We demonstrated here a method of exerting chemical control over insect flight activity, exploiting the use of immature stage implanted microfluidics to reversibly control the rate of metabolic output. Such a system could be the first step towards the development of an artificial insect nervous system where the controlled release of inhibitory or excitatory neurotransmitters could be accomplished in response to external stimuli. Extension of this work to include a multi-reservoir microfluidic device for short timescale release control (*i.e.* off/on/off/on) would enable a new paradigm for insect flight control alongside established electrical techniques.

Acknowledgements

This work was supported by the Defense Advanced Research Project Agency, Microsystems Technology Office, Hybrid Insect MEMS (HI-MEMS) program, through the Boyce Thompson Institute for Plant Research. Distribution unlimited. Fundamental research exempt from prepublication controls. The authors would like to thank Donn Kim, Likun Chen, Doo Hyung Lee, Dr Julie Goddard, Dr Frank Schroeder, Prof. John Ewer, Prof. James Marden and Prof. Amit Lal for helpful discussions and technical assistances. The facilities used for this research include Nanoscale Science & Technology Facility (CNF) and Nanobiotechnology Center (NBTC) at Cornell University.

References

- W. Shyy, M. Berg and D. Ljungqvist, *Prog in Aero Sci*, 1999, **35**, 455–505.
- Y. S. Lian, W. Shyy, D. Viieru and B. N. Zhang, *Prog in Aero Sci*, 2003, **39**, 425–465.
- M. Gad-el-Hak, *MEMS: Design and Fabrication*, CRC/Taylor & Francis Group, Boca Raton, FL, 2006.
- M. Tanaka, *Microelectron. Eng.*, 2007, **84**, 1341–1344.
- R. J. Wood, S. Avadhanula, E. Steltz, M. Seeman, J. Entwistle, A. Bachrach, G. Barrows, S. Sanders and R. S. Fearing, *IEEE Robot. Automat. Mag.*, 2007, **14**, 82–91.
- M. Gad-el-Hak, *J. Aircraft*, 2001, **38**, 419–429.
- D. J. Pines and F. Bohorquez, *J. Aircraft*, 2006, **43**, 290–305.
- C. P. Ellington, *J. Exp. Biol.*, 1999, **202**, 3439–3448.
- R. Wootton, *Nature*, 2000, **403**, 144–145.
- R. Dudley, *Science*, 1999, **284**, 1937–1939.
- N. Franceschini, F. Ruffier and J. Serres, *Curr. Biol.*, 2007, **17**, 329–335.
- R. J. Wood, *Proc IEEE/RSJ Int Conf Intelli Rob Sys*, 2007, 1889–1894.
- R. J. Wood, *IEEE Trans Robotics*, 2008, **24**, 341–347.
- R. J. Wood, S. Avadhanula, R. Sahai, E. Steltz and R. S. Fearing, *J. Mech. Design*, 2008, 130.
- H. Tanaka, K. Hoshino, K. Matsumoto and I. Shimoyama, *Proc IEEE/RSJ Int Conf Intelli Rob Sys*, 2005, 2706–2711.
- E. Steltz, S. Avadhanula and R. S. Fearing, *Proc IEEE/RSJ Int Conf Intelli Rob Sys*, 2007, 3987–3992.
- S. P. Sane, *J. Exp. Biol.*, 2003, **206**, 4191–4208.
- J. H. Marden, *J. Exp. Biol.*, 1987, **130**, 235–258.
- J. H. Marden, *J. Exp. Biol.*, 2005, **208**, 1653–1664.
- A. Bozkurt, R. Gilmour, D. Stern and A. Lal, *Proc 21st IEEE Int Conf MEMS*, 2008, 160–163.
- A. Bozkurt, A. Paul, S. Pulla, A. Ramkumar, B. Blossey, J. Ewer, R. Gilmour and A. Lal, *Proc 20th IEEE Int Conf MEMS*, 2007, 405–408.
- H. Sato, C. W. Berry, B. E. Casey, G. Lavella, Y. Ying, J. M. VandenBrooks and M. M. Maharbiz, *Proc 21st IEEE Int Conf MEMS*, 2008, 164–167.

-
- 23 N. Ando and R. Kanzaki, *Zool. Sci.*, 2004, **21**, 123–130.
- 24 R. E. Ritzmann, A. L. Ridgel and A. J. Pollack, *J. Comp. Physiol. A Neuroethol. Sens. Neural Behav. Physiol.*, 2008, **194**, 341–360.
- 25 T. Reissman and E. Garcia, *Adv in Sci Technol*, 2008, **58**, 159–164.
- 26 A. J. Chung, D. Kim and D. Erickson, *Lab Chip*, 2008, **8**, 330–338.
- 27 M. J. Owen and P. J. Smith, *J. Adhes. Sci. Tech.*, 1994, **8**, 1063–1075.
- 28 A. K. Sharma and H. Yasuda, *J. Vac. Sci. Technol.*, 1982, **21**, 994–998.
- 29 N. A. Alcantar, E. S. Aydil and J. N. Israelachvili, *J. Biomed. Mater. Res.*, 2000, **51**, 343–351.
- 30 A. Paul, A. Bozkurt, J. Ewer, B. Blossey and A. Lal, *Proc Solid State Sens Act Microsys Workshop*, 2006, 209–211.
- 31 R. F. Chapman, *The Insects: Structure and Function*, Cambridge University Press, New York, 1998.
- 32 H. F. Nijhout, *Insect Hormones*, Princeton University Press, New Jersey 1994.
- 33 A. J. Spence, K. B. Neeves, D. Murphy, S. Sponberg, B. R. Land, R. R. Hoy and M. S. Isaacson, *J. Neurosci. Methods*, 2007, **159**, 116–124.
- 34 L. D. Rash and W. C. Hodgson, *Toxicol.*, 2002, **40**, 225–254.
- 35 E. K. Michaelis, N. Galton and S. L. Early, *Proc. Natl. Acad. Sci. U. S. A.*, 1984, **81**, 5571–5574.
- 36 R. H. Osborne, *Pharmacol. Ther.*, 1996, **69**, 117–142.
- 37 J. T. Santini, M. J. Cima and R. Langer, *Nature*, 1999, **397**, 335–338.
- 38 G. C. Randall and P. S. Doyle, *Proc. Natl. Acad. Sci. U. S. A.*, 2005, **102**, 10813–10818.
- 39 J. H. Marden, B. Rogina, K. L. Montooth and S. L. Helfand, *Proc. Natl. Acad. Sci. U. S. A.*, 2003, **100**, 3369–3373.
- 40 J. F. Harrison and J. R. B. Lighton, *J. Exp. Biol.*, 1998, **201**, 1739–1744.